

PREDRAG KOJIĆ <sup>1</sup>  
JOVANA KOJIĆ <sup>2</sup>  
MILADA PEZO <sup>3</sup>  
JELENA KRULJ <sup>2</sup>  
LATO PEZO <sup>4</sup>  
NIKOLA MIRKOV <sup>3</sup>

<sup>1</sup> University of Novi Sad, Faculty of Technology Novi Sad, Novi Sad, Serbia

<sup>2</sup> University of Novi Sad, Institute of Food Technology, Novi Sad, Serbia

<sup>3</sup> University of Belgrade, Department of Thermal Engineering and Energy, "Vinča" Institute of Nuclear Sciences - National Institute of the Republic of Serbia

<sup>4</sup> University of Belgrade, Institute of General and Physical Chemistry, Belgrade, Serbia

#### SCIENTIFIC PAPER

UDC 532.5:519.6:66.021.2

## NUMERICAL STUDY OF THE HYDRODYNAMICS AND MASS TRANSFER IN THE EXTERNAL LOOP AIRLIFT REACTOR

### Article Highlights

- Numerical study of external-loop airlift reactor (ELAR) was performed
- Hydrodynamics and gas-liquid mass transfer coefficient of the ELAR was studied
- The influence of gas velocity, alcohol types and alcohol concentration were investigated
- A two-phase CFD model applying the Eulerian-Eulerian model was developed
- The coefficient of volumetric mass transfer was determined using CFD and ANN model

### Abstract

The objective of this study was to investigate the hydrodynamics and the gas-liquid mass transfer coefficient of an external-loop airlift reactor (ELAR). The ELAR was operated in three cases: different inlet velocities of fluids, different alcohols solutions (water, 0.5% methanol, 0.5% ethanol, 0.5% propanol and 0.5% butanol) and different concentration of methanol in solutions (0%, 0.5%, 1%, 2% and 5%). The influence of superficial gas velocity and various diluted alcohol solutions on hydrodynamics and the gas-liquid mass transfer coefficient of the ELAR was studied. Experimentally, the gas hold-up, liquid velocities and volumetric mass transfer coefficient values in the riser and the downcomer were obtained from the literature source. A computational fluid dynamics (CFD) model was developed, based on two-phase flow, investigating different liquids regarding surface tension, assuming the ideal gas flow, applying the finite volume method and Eulerian-Eulerian model. The volumetric mass transfer coefficient was determined using the CFD and artificial neural network model. The effects of liquid parameters and gas velocity on the characteristics of the gas-liquid mass transfer were simulated. These models were compared with the appropriate experimental results. The CFD model successfully simulates the influence of different alcohols regarding the number of C-atoms on hydrodynamics and mass transfer.

**Keywords:** airlift reactor, hydrodynamics, mass transfer, Eulerian-Eulerian model, artificial neural network model.

Airlift reactors are widely used in chemical engineering, process engineering, food industry and biotechnology, wastewater treatment, and various fermentation processes. Airlift reactors are gas-liquid or gas-liquid-solid contactors in which the gas is a dis-

persed phase and is introduced continuously. At the same time, the liquid is a continuous phase that is constantly introduced or in batches. The liquid circulates through separate tubes (riser and downcomer), and there is generally no recirculation of the gas phase. The advantages of these devices utilization are: mass and heat transfer are more efficient, high fluid circulation rate, simple construction with no moving parts, maintenance is easier, self-inducing fluid flow due to the difference of fluid densities in the riser and downcomer tube, reliable temperature control, good mixing and low production costs. The parameters that influence the working con-

Correspondence: L. Pezo, University of Belgrade, Institute of General and Physical Chemistry, Belgrade, Serbia.

E-mail: latopezo@yahoo.co.uk

Paper received: 22 May, 2021

Paper revised: 17 August, 2021

Paper accepted: 22 September, 2021

<https://doi.org/10.2298/CICEQ210522034K>

ditions are various: bubble size, the geometry of the construction, the temperature of the fluids, density, viscosity, surface tension, the rheological properties of the fluids, etc. Understanding these influences can contribute to a better conduct of output characteristics. The computational fluid dynamic (CFD) approach is a tool for mathematical modelling of complex flow characteristics and could be useful for this type of external loop airlift reactor. Different numerical approaches, such as artificial neural network (ANN) modelling, can also predict the mass transfer coefficient and hydrodynamic parameters.

The airlift reactor was firstly introduced in the study of Lefrancois *et al.* [1]. Then, a comprehensive review of the research concerning the investigations of the fluid physical characteristics, measurement techniques and review of the developed mathematical models of flow dynamics in airlift reactors were investigated by Zhang *et al.* [2].

For decades, engineers and researchers investigated the hydrodynamics and mass transfer in airlift reactors experimentally and numerically. Some proposed a modified construction of the airlift reactor to obtain better characteristics. A modified airlift reactor with slanted baffles in the riser compartment was developed to improve the oxygen transfer coefficient [3]. A construction based on a combination of an external loop airlift reactor with a fluidized bed was proposed in the study of Guo *et al.* [4]. Lukic *et al.* [5] proposed a novel design of self-agitated impellers to improve flow and mass transfer characteristics.

Many researchers dealt with experimental and numerical investigations to understand, analyse, and improve the flow regime and mass transfer in airlift reactors. The effect of the circulation liquid velocity and the influence of the riser-to-downcomer cross-sectional area ratio on the mixing efficiency was investigated both experimentally and numerically in the study by Burlutskii and Felice [6]. The analyses of the mass transfer in an external-loop airlift reactor were presented in many literature reports [7-10]. The two-phase mathematical model with turbulence characteristics has been used to predict the overall mass transfer coefficient. Experimental analyses and mathematical models have been developed to predict the axial dispersion coefficient in the riser of an external-loop airlift reactor [11].

Experimental study of the hydrodynamics of the liquid circulation was investigated in many literature reports [12, 13]. It was shown that the transition between the homogeneous and heterogeneous flow regimes depends on the liquid circulation, initial gas distribution, and equipment size. The determination

mass transfer coefficient and prediction of the volumetric oxygen transfer coefficient were analyzed in experiments performed by numerous authors [14, 15]. Lin *et al.* [16] investigated the influence of the gas distributor on the local hydrodynamic behaviour of an external loop airlift reactor. Pronczuk and Bizon [17] performed an experimental study of the liquid mixing characteristic of an external-loop airlift reactor with a fluidized bed.

Several computational two-phase flow models can be found in the literature. Jiang *et al.* [18] introduced a CFD study with three different drag models. McClure *et al.* [19] developed a computational numerical model of surfactant-containing systems. The computational approach introduced by the Eulerian-Eulerian model has been introduced with the standard  $k-\varepsilon$  turbulence model [20, 21]. Roy *et al.* [22] performed the CFD simulation using the two-fluid flow and axial dispersion model in external loop airlift reactors. A two-phase turbulent  $k-\varepsilon$  computational model considering the drag, lift, and turbulent dispersion forces was used to model an airlift loop reactor to treat refined soybean oil wastewater [23]. Other numerical methods have also been used for modelling flow in the airlift reactors, such as the model based on macroscopic balances of the external loop airlift reactor operating in three stages [24], the model supported by vector regression for predicting hydrodynamic parameters [25], and the artificial neural network model for predicting mass transfer in external loop airlift reactors [26].

In this paper, analyses of the hydrodynamics and gas-liquid mass transfer coefficient of airlift reactor were investigated for: water as working fluid, with different superficial gas inlet velocities (0.01-0.08 m/s) (the first set of experiments, which showed the influence of the superficial gas velocity); different working fluids, including water, 0.5% methanol, 0.5% ethanol, 0.5% propanol and 0.5% butanol (the second set of experiments, which showed the influence of the fluid type); and different methanol concentration in water, 0% methanol, 0.5% methanol, 1% methanol, 2% methanol and 5% methanol (the third set of experiments, which showed the influence of fluid concentration). The experimental results [27] were compared with the developed computational model. The two-phase Eulerian-Eulerian model was used for the numerical experiments, and the standard  $k$ -approach was used to model turbulence characteristics. It is worth noting that there is no record in the scientific literature that researchers have succeeded to simulate the influence of various aliphatic alcohols with different concentrations on the hydrodynamics in ELAR systems. Therefore, one of the objectives of this study was to investigate the possibility of predicting the gas hold-up

and gas-liquid mass transfer coefficient for three sets of experiments using the ANN model.

## MATERIALS AND METHODS

The experiment results were taken from a study by Posarac [27] and used for CFD modelling. The diameter of the riser and downcomer was 0.10 m, and the tube height was 2.83 m. Complete separation of the gas and liquid phases occurred in the upper part of the column. Subsequently, the gas did not circulate through the downcomer. The air was sparged in the column through a single orifice of 4 mm in diameter. In all experiments, compressed air was used as the gas phase. The experimental considerations were designed for different inlet velocities (between 0.01 and 0.08 m/s) (first experiment), five types of fluids in the second experiment (water, 0.5% methanol, 0.5% ethanol, 0.5% propanol and 0.5% butanol), and five different methanol concentrations in the third experiment (0% methanol, 0.5% methanol, 1% methanol, 2% methanol and 5% methanol). The physical properties of these liquids are given in Table 1.

Table 1. Properties of the fluids at 20 °C (Posarac, 1988)

Liquid phase	Density (kg/m <sup>3</sup> )	Viscosity (mPa·s)	Surface tension (mN/m)
Water	999.7	1.31	74.2
0.5% methanol	999.0	1.20	72.1
0.5% ethanol	998.8	1.20	70.1
0.5% propanol	998.5	1.21	68.3
0.5% butanol	994.9	1.21	63.8
1% methanol	998.0	1.20	69.9
2% methanol	996.2	1.19	67.2
5% methanol	993.0	1.17	61.6

Experimental tests within this research [27] include the measurements of gas hold-up in the riser tube, the determination of liquid velocity in the downcomer, and the volumetric mass transfer coefficient for the above-mentioned model systems in the ELAR.

The geometrical characteristics of this airlift reactor were presented in the literature [27]. The basic geometry parameters used for the CFD simulation were: the riser tube diameter and height (100 mm and 2800 mm, respectively), the downcomer tube diameter and height (100 mm and 1950 mm, respectively), and the separator width, length and height (300 mm, 440 mm, and 280 mm, respectively), while the gas inlet

diameter was 4 mm. In addition, the distance between the riser and downcomer tube was 100 mm, the liquid height above the inlet tube was 40 mm, and the volume of the liquid was approximately 45 l. The ELAR schematic diagram and the 3D model used for computational simulations are presented in Figure 1.

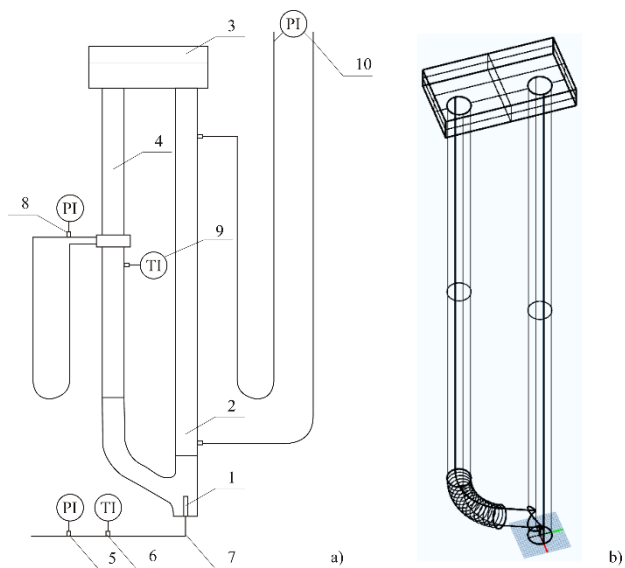


Figure 1. External loop airlift reactor; a) schematic diagram of external loop airlift reactor, 1-inlet, 2-riser tube, 3-gas separator, 4-downcomer tube, 5-manometer, 6-thermometer, 7-gas flow meter, 8-manometer, 9-thermometer, 10-manometer, b) 3D model used for computational simulations.

## Description of the computational model

The numerical experiments were performed to determine the potential of fluid velocity, gas hold-up and gas-liquid mass transfer coefficient for different inlet superficial gas velocities, five fluid types, and different alcohol concentrations, as mentioned in the experimental study section. The Eulerian-Eulerian multiphase model simulated the flow regime in the considered airlift reactor. In the Euler-Euler approach, the different phases were treated as interpenetrating fluids. Each phase occupies its volume, which a different phase cannot occupy. Therefore, the phasic volume fraction concept was introduced and was a distinguishing feature of the model. Conservation equations for momentum and continuity for each phase were solved separately, having a similar structure for all phases. These equations were closed by using constitutive correlations obtained from empirical data. Conservation equations were coupled with the pressure field, which was the same for all phases and through interphase exchange coefficients. In the presented model, the action of the gravitational force was also assumed and added to the balance equations.

## Governing equations

The mass conservation equation for a phase identified by an index  $k$  has the following form:

$$\frac{\partial}{\partial t}(\alpha_k \rho_k) + \nabla \cdot (\alpha_k \rho_k \vec{v}_k) = 0 \quad (1)$$

where  $\vec{v}_k$  and  $\rho_k$  are the velocity and density of phase  $k$ . The parameter  $\alpha_k$  represents the void fraction of phase  $k$ .

The momentum conservation equation for a phase identified by index  $k$  has the following form:

$$\begin{aligned} \frac{\partial}{\partial t}(\alpha_k \rho_k \vec{v}_k) + \nabla \cdot (\alpha_k \rho_k \vec{v}_k \vec{v}_k) = \\ -\alpha_k \nabla p + \nabla \cdot \tau_k + \alpha_k \rho_k \vec{g} + \vec{F}_k + \vec{F}_{i,k} + \vec{F}_{lift,k} + \vec{F}_{vm,k} \end{aligned} \quad (2)$$

where  $\nabla p$  is the gradient of the shared pressure,  $\tau_k$  is the stress tensor,  $\vec{F}_k$  is external body force,  $\vec{F}_{i,k}$  is the interphase drag force,  $\vec{F}_{l,k}$  is the lift force, and  $\vec{F}_{vm,k}$  is the virtual mass force.

The stress-strain tensor  $\tau_k$  was computed by:

$$\tau_k = \alpha_k \mu_k (\nabla \vec{v}_k + \nabla \vec{v}_k^T) + \alpha_k \left( \lambda_k - \frac{2}{3} \mu_k \right) \nabla \cdot \vec{v}_k \quad (3)$$

where  $\mu_k$  is shear, and  $\lambda_k$  is the bulk viscosity of phase  $k$ .

Interphase exchange is usually modelled by the Schiller and Naumann drag model [28]. However, this model is usually used for the particles in still fluids. When applied to the external loop reactor, it needs to be modified. This correlation has been widely used to simulate gas-liquid flow [29, 20]; it considers the spherical shape and uniform gas bubble size. A bubble diameter of 3.0 mm was reasonable to approach the flow pattern [20].

The lift force was calculated by [30]:

$$\vec{F}_{lift,k} = -0.5 \rho_k \alpha_k (\vec{v}_k - \vec{v}_j) \times (\nabla \times \vec{v}_k) \quad (4)$$

Virtual mass force was defined in the following manner:

$$\vec{F}_{vm} = 0.5 \rho_k \alpha_k \left( \frac{d\vec{v}_k}{dt} - \frac{d\vec{v}_j}{dt} \right) \quad (5)$$

## Coefficients of mass transfer

The volumetric mass transfer coefficient is calculated as the product of the overall mass transfer coefficient and specific interfacial area. The specific interfacial area depends on the bubble diameter and gas hold-up values. The overall mass transfer coefficient depends on the diffusivity of oxygen in the water and the contact time [9, 31]. The model of mass transfer coefficient based on penetration theory [32]

has been compared for all experimental conditions. The results showed that the penetration model predicts mass transfer coefficient values slightly higher. Regarding other details of the solution algorithm, the choices of the particular schemes, based on previous experience, the suggestion from official software documentation, and the published literature, are summarized in Table 2.

Table 2. Simulation settings

Solver type	Pressure based, 3D, transient
Multiphase model	Eulerian, no slip velocity
Viscous model	Turbulent, two-equation standard $k-\epsilon$
Materials	Primary phase-water, 0.5% methanol, 0.5% ethanol, 0.5% propanol and 0.5% butanol (the second set of experiments); Water, 0.5% methanol, 1% methanol, 2% methanol and 5% methanol butanol (the third set of experiments); Secondary phase-air
Interaction between phases	Schiller and Naumann (Schiller and Naumann, 1935)
Pressure-velocity coupling	SIMPLE
Pressure interpolation scheme	PRESTO!
Convection scheme - momentum	Second order upwind
Turbulent scalars	First order upwind
Volume fraction	Second order upwind
Time stepping	Backward Euler, first order

Boundary conditions were defined in the following manner: air inlet (0.01-0.08 m/s), fixed walls, an outlet at the top of the reactor, atmospheric pressure. At the inlet, the flow rate conditions were defined as the values of the inlet velocity (constant), the turbulence intensity was set to 5% (constant), and the inlet hydraulic diameter (constant). No-slip velocity conditions were used as boundary conditions at the fixed walls [9, 20]. A special class of the boundary condition was used at the outlet, where the turbulence intensity was set to 5% and the outlet hydraulic diameter was constant. The computational domain was large enough for boundary conditions and did not affect the liquid flow characteristics. The reference values were 300 kPa for pressure and 293 K for temperature. It was assumed that the bubble diameter was 3 mm, and it was an acceptable size to predict the flow pattern in the vicinity of the bulk zone [20, 33]. It was also assumed that the

bubbles have approximately the same size [39]. The time step was 0.001 s.

The three-dimensional computational mesh was used to represent the experimental domain. The presented mesh consisted of tetrahedral cells, with around 900,000 cells. Repeated simulations were conducted on the successively refined meshes until the desired mesh independence was observed, and the reported results were pertinent to the grid-independent solutions. The convergence was achieved when the sums of the absolute values of the residuals for all variables fell below  $10^{-5}$ . Numerical mesh refinement tests showed that the gas hold-up and the overall flow field predictions were relatively insensitive to the increase of the control volumes.

The system of the governing equations introduced the numerical investigation. First, the balance equation set was solved using the finite control volume method based on the SIMPLE solution method (Semi-Implicit Method for Pressure Linked Equations, [34]). Then, a discretization of the partial differential equations for momentum, volume fraction, turbulent kinetic energy, and transient formulation was carried out by the second-order upwind spatial discretization method. The numerical simulations were performed in Ansys Fluent computer code.

### ANN modelling

A multi-layer perceptron model (MLP), which consisted of three layers (input, hidden, and output), was used for modelling an artificial neural network model (ANN) for the prediction of gas hold-up and gas-liquid mass transfer coefficient. Before the calculation, both input and output data were normalized to improve the behaviour of the ANN [35, 36]. In addition, the Broyden-Fletcher-Goldfarb-Shanno (BFGS) algorithm was used as an iterative method for solving unconstrained nonlinear optimization during the ANN modelling.

The experimental database for ANN was randomly divided into training, cross-validation, and testing data (with 60%, 20%, and 20% of experimental data, respectively). A series of different topologies were used, in which the number of hidden neurons varied from 5 to 20, and the training process of the network was run 100,000 times with random initial values of weights and biases. Coefficients associated with the hidden layer (weights and biases) were grouped in matrices  $W_1$  and  $B_1$ . Similarly, coefficients related to the output layer were grouped in matrices  $W_2$  and  $B_2$  [37]:

$$Y = f_1(W_2 \cdot f_2(W_1 \cdot X + B_1) + B_2) \quad (6)$$

where:  $Y$  is the matrix of the output variables,  $f_1$  and  $f_2$  are transfer functions in the hidden and output layers, respectively, and  $X$  is the matrix of input variables.

The coefficients of determination were used as parameters to check the performance of the obtained ANN model.

### The accuracy of the model

The numerical verification of the developed model was tested using the coefficient of determination ( $R^2$ ), reduced chi-square ( $\chi^2$ ), mean bias error (MBE), root mean square error (RMSE) and mean percentage error (MPE). These commonly used parameters can be calculated as follows [38]:

$$\begin{aligned} \chi^2 &= \frac{\sum_{i=1}^N (x_{\text{exp},i} - x_{\text{pre},i})^2}{N - n}, \\ RMSE &= \left[ \frac{1}{N} \cdot \sum_{i=1}^N (x_{\text{pre},i} - x_{\text{exp},i})^2 \right]^{1/2}, \\ MBE &= \frac{1}{N} \cdot \sum_{i=1}^N (x_{\text{pre},i} - x_{\text{exp},i}), \\ MPE &= \frac{100}{N} \cdot \sum_{i=1}^N \left( \frac{|x_{\text{pre},i} - x_{\text{exp},i}|}{x_{\text{exp},i}} \right) \end{aligned} \quad (7)$$

where  $x_{\text{exp},i}$  stands for the experimental values and  $x_{\text{pre},i}$  are the predicted values calculated by the model, and  $N$  and  $n$  are the number of observations and constants, respectively.

## RESULTS AND DISCUSSION

The operation of ELAR was influenced by hydrodynamic parameters related to the behaviour of gas bubbles, such as bubble size, bubble velocity, liquid velocity, etc. Bubble formation has two stages: expansion and bubble rising [39,40]. According to that, the size of the bubble in the bubble flow was determined by the thrust force and interphase stress forces, in the transient flow by the instability of the gas-liquid surface, and at high gas velocities, in the turbulent flow by the ratio of dynamic pressure forces to surface tension forces. With a large number of bubbles, the bubble velocity was small due to the bubbles' mutual interference and the liquid's return flow.

### CFD model

The 3D numerical simulations were conducted, and the results of those numerical experiments are validated with experimental results of gas hold-up and

the velocities of the liquid phase [27].

The computational modelling results for the water velocity field and the superficial gas velocities of 0.01, 0.03, 0.05 and 0.07 m/s are shown in Figure 2. The recirculation of the liquid phase could be observed for all the observed superficial velocities in all cases. The higher value of superficial velocity induced the augmented velocities in both riser and downcomer tubes and recirculation rates. The flow from the downcomer tube strongly influenced the turn of the liquid flow at the position where the downcomer and the riser tube collides.

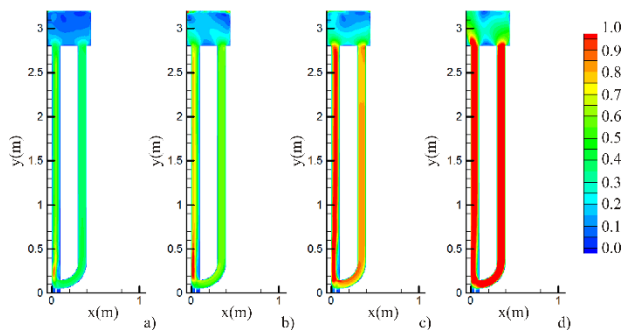


Figure 2. Overall water velocity contours for the superficial velocity of gas: a) 0.01 m/s, b) 0.03 m/s, c) 0.05 m/s and d) 0.07 m/s.

The effect of the dissolved alcohols in water on velocity profile was shown in Figure 3 for water, 0.5% methanol, 0.5% ethanol, 0.5% propanol, and 0.5% butanol. Again, the minimum flow pattern was observed for water. At the same time, the last two cases (0.5% propanol and 0.5% butanol) showed the maximum liquid flow velocities (which were reached according to lesser density and viscosities).

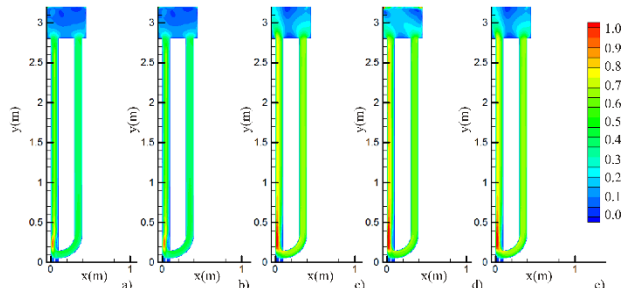


Figure 3. Overall fluid velocity contours for the superficial velocity of gas (equal to 0.01 m/s): a) water, b) 0.5% methanol, c) 0.5% ethanol, d) 0.5% propanol, and e) 0.5% butanol.

The influence of the alcohol concentration (0.5% methanol, 1.0% methanol, 2.0% methanol and 5.0% methanol) was presented on Figure 4. The higher concentration of methanol in the solution influenced

the increase of the velocity in the liquid phase. The aliphatic alcohols (ethanol, propanol and butanol) behave similarly, which coincide with the research by Keitel [41], who showed that a minimum and upper limiting alcohol concentration exerted a noticeable effect on the hydrodynamics and liquid velocity. Increasing the alcohol concentration above the upper limiting concentration enhances the liquid phase frothing and bubble coalescence effect. Therefore, with coalescence prevention in the riser, the driving force for liquid circulation decreased due to a large number of small bubbles representing the resistance to circulation [42].

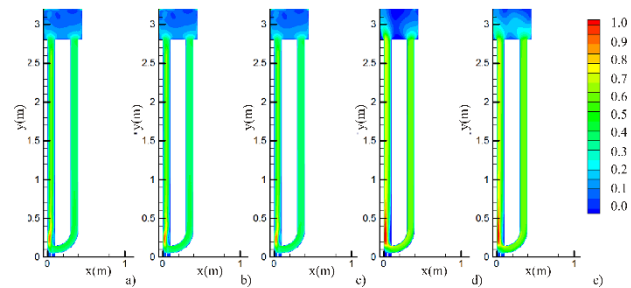


Figure 4. Overall fluid velocity contour for the superficial velocity of gas (equal to 0.01 m/s): a) water, b) 0.5% methanol, c) 1.0% methanol, d) 2.0% methanol, and e) 5.0% methanol.

It can be seen that the increase of the superficial gas velocity induces the increase of the gas hold-up and the swell level position, Figure 5. Therefore, according to the CFD results, there was no gas phase in the downcomer tube, which the experiments confirmed [27].

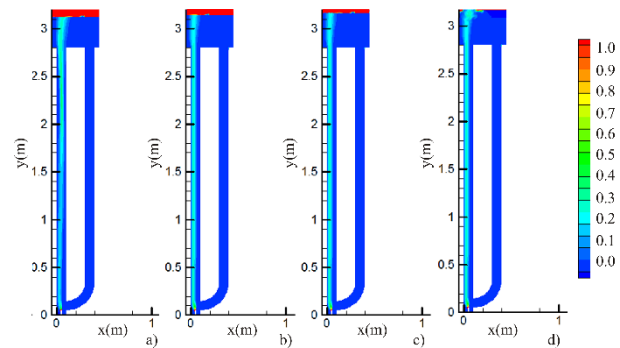
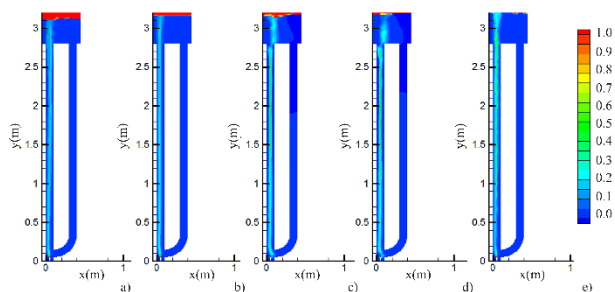


Figure 5. Overall gas hold-up contours for the superficial velocity of gas: a) 0.01 m/s, b) 0.03 m/s, c) 0.05 m/s and d) 0.07 m/s for water.

In Figure 6, the gas hold-up profiles for different fluids were presented. The liquid type (water, or methanol, ethanol, propanol or butanol solution) affected the swell level and the gas hold-up profile. The maximum gas hold-up was observed for 0.5% butanol solution, which was also gained for experimental investigation. The results showed that the increase of

the surface tension gradient, as a consequence of alcohol addition, strongly impacts the airlift reactor's hydrodynamics and mass transfer characteristics. The increase of the surface tension gradient corresponds to the rise of the number of carbon atoms in alcohol molecules [42–44]. The alcohol addition has a remarkable effect on the gas holdup. For example, gas holdup values have an average increase of about 39%, 43%, 70%, and 60% when alcohol solutions (methanol, ethanol, propanol, and butanol, respectively) were added, compared to water. The gas holdup increase was noticeable for the superficial gas velocities up to 0.03 m/s. When the fully turbulent regime was achieved, the alcohol addition did not affect the coalescence prevention, which produced a lower gas holdup increase (about 30%). The alcohol addition has a smaller effect on the liquid velocity than on the gas holdup, and the liquid velocity increased about 10% with alcohol addition.



*Figure 6. Overall gas hold-up contours for the superficial velocity of gas (equal to 0.01 m/s): a) water, b) 0.5% methanol, c) 0.5% ethanol, d) 0.5% propanol, and e) 0.5% butanol.*

In Figure 7, the methanol concentration was investigated, and the gas hold-up was increased at a higher methanol concentration in the water solution. It has been perceived that the influence of alcohols on gas holdup increases with the augment of their concentration and the length of the carbon chain in the alcohol molecule [43]. It can be explained by changes in the surface tension gradient that causes the different coalescence suppression strengths of specific alcohol. Therefore, alcohols with lower C-atoms show lower surface tension gradients and produce lower gas holdup values [44]. In the same manner, surface tension decrease with the augment of alcohol concentration while surface tension gradient rises and consequently leads to an increase in the gas holdup of the ELAR.

In Figure 8, the experimental and CFD-predicted results for gas hold-up values are compared. For predicting gas hold-up for water, 0.5% methanol, 0.5% ethanol, 0.5% propanol, and 0.5% butanol, the CFD

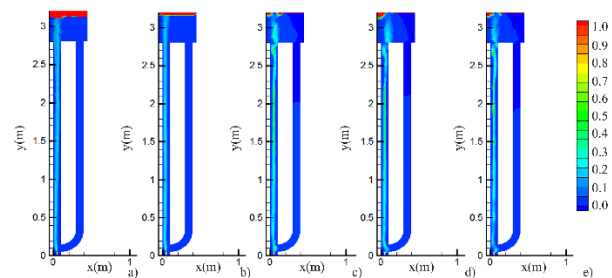


*Figure 7. Overall gas hold-up contours for the superficial velocity of gas (equal to 0.01 m/s): a) water, b) 0.5% methanol, c) 1.0% methanol, d) 2.0% methanol, and e) 5.0% methanol.*

model showed a good prediction capability, as can be visually observed in Figure 8a. The deviations that can be seen were attributed to the relative inaccuracy of the physical parameters of the solutions. The prediction capabilities of these models could be accessed in Table 3 ( $r^2$  values were 0.995; 0.993; 0.995; 0.991 and 0.997, respectively). According to the CFD model for the prediction of gas hold-up for water, 0.5% methanol, 1% methanol, 2% methanol and 5% methanol, the predicted variables were: 0.998; 0.996; 0.998; 0.996 and 0.992, respectively, Figure 8b and Table 3.

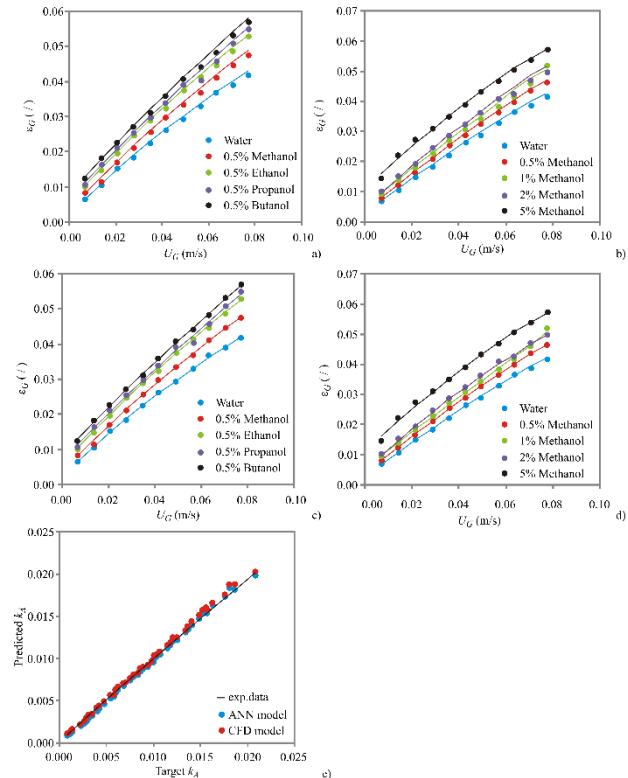


*Figure 8. Comparison of experimentally obtained gas hold-up (presented as dots) for water, 0.5% methanol, 0.5% ethanol, 0.5% propanol and 0.5% butanol with a) CFD model and b) CFD model, prediction of gas hold-up for water, 0.5% methanol, 1% methanol, 2% methanol and 5% methanol with c) ANN model and d) ANN model and e) prediction coefficient of volumetric mass transfer (model data are presented as lines).*

Table 3. The "goodness of fit" tests for the developed models

CFD models , for the prediction of gas hold- up										
	$\chi^2$	RMSE	MBE	MPE	$r^2$	Skew	Kurt	Mean	StDev	Var
Water	8.16E-07	8.61E-04	3.07E-04	2.290	0.995	-0.700	2.118	0.000	0.001	7.13E-07
Methanol, 0.5%	1.28E-06	1.08E-03	-2.98E-04	2.784	0.993	1.494	3.013	0.000	0.001	1.18E-06
Ethanol, 0.5%	1.13E-06	1.01E-03	-1.84E-04	2.563	0.995	-0.241	-0.076	0.000	0.001	1.09E-06
Propanol, 0.5%	2.17E-06	1.40E-03	2.17E-05	2.526	0.991	0.639	0.078	0.000	0.001	2.16E-06
Butanol, 0.5%	1.27E-06	1.07E-03	-6.62E-04	2.164	0.997	-0.477	-1.279	-0.001	0.001	7.84E-07
Water	9.06E-07	9.08E-04	-6.09E-04	2.783	0.998	0.353	-1.503	-0.001	0.001	4.98E-07
Methanol, 0.5%	7.68E-07	8.35E-04	2.52E-04	2.066	0.996	0.793	-0.283	0.000	0.001	6.98E-07
Methanol, 1%	1.82E-06	1.28E-03	-8.38E-04	2.870	0.998	-0.295	-1.232	-0.001	0.001	1.04E-06
Methanol, 2%	9.49E-07	9.29E-04	-1.37E-04	2.007	0.996	-1.409	1.867	0.000	0.001	9.29E-07
Methanol, 5%	1.56E-06	1.19E-03	2.10E-04	2.427	0.992	-0.406	-0.512	0.000	0.001	1.51E-06
ANN model, for prediction of gas hold- up (MLP 1-5-5 and MLP 1-4-5)										
Water	2.15E-06	1.08E-03	-5.47E-04	6.467	0.996	-0.585	0.820	-0.001	0.001	9.62E-07
Methanol, 0.5%	1.70E-06	9.62E-04	-3.40E-04	4.823	0.998	-0.616	0.056	0.000	0.001	8.92E-07
Ethanol, 0.5%	1.54E-06	9.17E-04	-1.99E-04	3.576	0.997	-2.157	5.625	0.000	0.001	8.81E-07
Propanol, 0.5%	2.97E-06	1.27E-03	-5.49E-04	4.772	0.994	-1.142	1.249	-0.001	0.001	1.45E-06
Butanol, 0.5%	2.47E-06	1.16E-03	-3.69E-04	3.793	0.995	-1.411	1.428	0.000	0.001	1.33E-06
Water	2.74E-07	3.86E-04	3.74E-05	1.409	0.999	1.091	1.285	0.000	0.000	1.63E-07
Metanol, 0.5%	6.05E-08	1.82E-04	3.01E-05	0.756	1.000	-0.233	-1.176	0.000	0.000	3.53E-08
Metanol, 1%	9.81E-07	7.32E-04	6.07E-05	2.643	0.997	0.175	-0.788	0.000	0.001	5.85E-07
Metanol, 2%	3.17E-07	4.16E-04	1.55E-05	1.037	0.999	-0.987	1.969	0.000	0.000	1.90E-07
Metanol, %5	9.57E-07	7.22E-04	-8.56E-05	2.255	0.997	0.150	0.342	0.000	0.001	5.66E-07
ANN model for prediction of gas-liquid mass transfer coefficient in methanol solution (MLP 6-8-1)										
$k_A$	3.9E-08	0.000	4.8E-06	3.115	0.999	1.313	4.889	4.8E-06	2E-04	3.9E-08

**ANN model**

The results of the experiments and results of the ANN models prediction (MLP 1-5-5) for gas hold-up values were presented in Figure 8c (gas hold-up for water, 0.5% methanol, 0.5% ethanol, 0.5% propanol

and 0.5% butanol) and Figure 8d, for model MLP 1-4-5 (gas hold-up for water, 0.5% methanol, 1% methanol, 2% methanol and 5% methanol), which showed good prediction capabilities. The prediction capabilities of these models could be accessed in Table 3 and 4.

Table 4. Artificial neural network model summary (performance and errors), for training, testing, and validation cycles

Network name	Performance			Error			Training algorithm	Error function	Hidden activation	Output activation
	Train.	Test.	Valid.	Train.	Test.	Valid.				
MLP 1-5-5	0.998	1.000	1.000	0.000	0.000	0.000	BFGS 18	SOS	Tanh	Exponential
MLP 1-4-5	0.999	1.000	1.000	0.000	0.000	0.000	BFGS 51	SOS	Tanh	Identity
MLP 6-8-1	0.999	1.000	1.000	0.000	0.000	0.000	BFGS 100	SOS	Logistic	Tanh

\* Performance term represents the coefficients of determination, while error terms indicate a lack of data for the ANN model.

The ANN models predicted experimental variables reasonably well for a broad range of the process variables. The ANN model had an insignificant lack of fit tests, which means the model satisfactorily predicted output variables. A high  $r^2$  indicates that the variation was accounted for and that the proposed model fitted the data adequately [45, 46].

### Coefficients of mass transfer

The ANN model performance for prediction of gas-liquid mass transfer coefficient in water, 0.5% methanol, 0.5% ethanol, 0.5% propanol and 0.5% butanol (MLP 6-8-1) was presented in Table 4. This model predicts the gas-liquid mass transfer coefficient well (the  $r^2$  values during the training cycle for the output variable were 0.999, Table 3).

The goodness of fit between experimental measurements and model-calculated outputs, represented as ANN performance (sum of  $r^2$  between measured and calculated output variables), during training, testing and validation steps, are shown in Table 3, while the visual confirmation of the ANN model could be observed in Figure 8e. The gas holdup and mass transfer coefficients are similar to other research [43, 44].

### CONCLUSION

Analyses of the hydrodynamics and mass transfer in the external loop airlift reactor were performed. The analyses were performed for different superficial gas velocities and two experimental sets depending on the type and concentration of alcohol solutions (working fluids). In addition, the values of gas hold-up, liquid velocity and volumetric mass transfer were compared with experimental values obtained from the literature [27].

The higher superficial inlet gas velocity increased the liquid velocity in both riser and downcomer tubes and recirculation rates. The minimum flow was observed for water, while the higher molecular weight alcohols increased the liquid velocity. Moreover, the higher diluted alcohol concentration influenced the increase of the velocity in the liquid phase.

The increase of the superficial inlet gas velocity induces the increase of the gas hold-up and the increase of the swell level position. The flow from the downcomer tube strongly influenced the profile of the liquid flow at the collision point of the downcomer and the riser tubes. According to the CFD results, there was no gas phase in the downcomer tube, which was also confirmed by the experiments. The liquid type affected the swell level position and gas hold-up profile. The maximum gas hold-up was observed for the highest

investigated molecular weight alcohol, also gained for the experimental investigation. The gas hold-up was increased for a higher alcohol concentration in the water solution.

CFD and ANN results for the volumetric mass transfer coefficient showed good agreement with experimental results.

### Acknowledgment

The research is funded by the Ministry of Education, Science and Technological Development of the Republic of Serbia No. 451-03-9/2021-14/ 200051 and Serbian-Slovenian bilateral project No. 337-00-21/2020-09/40.

### NOMENCLATURE

$C_D$	drag coefficient
$\vec{F}_{i,k}$	interphase drag force
$\vec{F}_{l,k}$	lift force
$\vec{F}_k$	external body force
$\vec{F}_{vm,k}$	virtual mass force
$p$	pressure (Pa)
Re	Reynolds number
$\vec{R}_{jk}$	interaction force between phases
$r^2$	coefficient of determination
$t$	time (s)
$T$	temperature (°C)
$v$	velocity (m/s)
$x_{exp,i}$	experimental values
$x_{pre,i}$	the predicted values calculated by the model
$N$	number of observations
$n$	number of constants
$a_k$	void fraction of phase $k$
$\lambda_k$	bulk viscosity of phase $k$
$\mu_k$	shear
$\rho$	density (kg/m <sup>3</sup> )
$\tau_k$	the stress tensor
$\chi^2$	reduced chi-square
ANN	Artificial Neural Network
CFD	Computational Fluid Dynamics
ELAR	External-Loop Airlift Reactor
FVM	Finite Volume Method
MBE	Mean Bias Error
MLP	Multi-Layer Perceptron Model

MPE	Mean Percentage Error
RMSE	Root Mean Square Error
SIMPLE	Semi-Implicit Method for Pressure Linked Equations

## REFERENCES

- [1] M.L. Lefrancois, C.G. Mariller, J.V. Mejane, Effectiveness aux procedes de cultures forgiques et de fermentations industrielles. Brevet d'Invention, France, no. 1 102 200. (1955).
- [2] T. Zhang, C. Wei, C. Feng, Y. Ren, H. Wu, S. Preis, Chemical Engineering & Processing: Process Intensification. 144 (2019) 107633.
- [3] S. Bun, N. Chawaloeshponiya, F. Nakajima, T. Tobino, P. Painmanakul, Journal of Environmental Chemical Engineering, 7 (2019) 103206.
- [4] Y.X. Guo, Rathor, M.N., Ti, H.C., Chem. Eng. J. 67 (1997) 205-214.
- [5] N. Lj. Lukic, I. M. Sijacki, P. S. Kojic, S. S. Popovic, M. N. Tekic, D. Lj. Petrovic, Biochem. Eng. J. 118 (2017) 53-63.
- [6] E. Burlutskii, R. Di Felice, Int. J. of Multiphas. Flow 119 (2019) 1-13.
- [7] H. Dhaouadi, S. Poncin, J. M. Hornut, G. Wild, P. Oinas, J. Korpijarvi, Chem. Eng. Sci. 52 (1997) 3909- 3917.
- [8] P. Lestinsky, P. Vayrynen, M. Vecer, K. Wichterle, Procedia Engineer. 42 (2012) 892 - 907.
- [9] S. M. Teli, C. Mathpati, Chinese J. Chem. Eng. 32 (2021) 39-60.
- [10] R. Salehpour, E. Jalilnejad, M. Nalband, K. Ghasemzadeh, Particuology. 51 (2020) 91-108.
- [11] Ch. Vial, S. Poncin, G. Wild, N. Midoux, Chem. Eng. Sci. 60 (2005) 5945 - 5954.
- [12] A.H. Essadki, B. Gourich, Ch. Vial, H. Delmas, Chem. Eng. Sci. 66 (2011) 3125-3132.
- [13] N. Bendjaballah, H. Dhaouadi, S. Poncin, N. Midoux, J. M. Hornut, G. Wild, Chem. Eng. Sci. 54 (1999) 5211-5221.
- [14] M. Gavrilescu, R. Z. Tudose, Chem. Eng. J. 66 (1997) 97-104.
- [15] K. Mohanty, D. Das, M. N. Biswas, Chem. Eng. J. 133 (2007) 257-264.
- [16] J. Lin, M. Han, T. Wang, T. Zhang, J. Wang, Y. Jin, Chem. Eng. J. 102 (2004) 51-59.
- [17] M. Pronczuk, K. Bizon, Chem. Eng. Sci. 210 (2019) 115231.
- [18] X. Jiang, N. Yang, B. Yang, Particuology 27 (2016) 95-101.
- [19] D. D. McClure, H. Norris, J. M. Kavanagh, D. F. Fletcher, G. W. Barton, Chem. Eng. Sci. 127 (2015) 189-201.
- [20] N. Moudoud, R. Rihani, F. Bentahar, J. Legrand, Chemical Engineering & Processing: Process Intensification 129 (2018) 118-130.
- [21] K. M. Dhanasekharan, J. Sanya, A. Jain, A. Haidari, Chem. Eng. Sci. 60 (2005) 213 - 218.
- [22] S. Roy, M. T. Dhotre, J. B. Joshi, Chem. Eng. Res. Des. 84(A8) (2005) 677-690.
- [23] Y. Shi, S. Wu, H. Ren, M. Jin, L. Wang, N. Qiao, D. Yu, Bioresource Technol. 296 (2020) 122316.
- [24] S. Sarkar, K. Mohanty, B.C. Meikap, Chem. Eng. J. 145 (2008) 69-77.
- [25] P. Kojic, R. Omorjan, Chem. Eng. Res. Des. 125 (2017) 398-407.
- [26] N. Naidoo, W.J. Pauck, M. Carsky, South African Journal of Chemical Engineering 33 (2020) 83-89.
- [27] D. Posarac, Investigation of Hydrodynamics and Mass-transfer in External-loop Airlift Reactor. University of Novi Sad, Faculty of Technology, Novi Sad, Serbia (PhD) (1988).
- [28] L. Schiller, A. Naumann,.. VDI Zeitung, 77 (1935) 318-320.
- [29] A. Gupta, S. Roy, Chem. Eng. J. 225 (2013) 818-836.
- [30] A. Tomiyama, G.P. Celata, S. Hosokawa, S. Yoshida, Int. J. Multiph. Flow. 28 (2002) 1497-1519.
- [31] X. Lu, J. Yu, Y. Ding, Can J Chem Eng 98(7) (2020) 1593-1606.
- [32] R. Higbie, Trans. Am. Inst. Chern. Eng. 31 (1935) 365-389.
- [33] M. Pourtousi, P. Ganesan, J.N. Sahu, Measurement 76 (2015) 255-270.
- [34] S.V. Patankar, D.B. Spalding, Int. J. Heat Mass Transfer 15 (1972) 1787-1806.
- [35] T. Kollo, D. von Rosen, Advanced Multivariate Statistics with Matrices (Springer, Dordrecht) (2005).
- [36] L. Pezo, B.Lj. Ćurčić, V.S. Filipović, M.R. Nićetin, G.B. Koprivica, N.M. Mišjenović, Lj.B. Lević, Hem. Ind. 67 (2013) 465-475.
- [37] C.I. Ochoa-Martinez, A.A. Ayala-Aponte, LWT - Food Sci Technol 40 (4) (2007) 638-6.
- [38] M. Aćimović, L. Pezo, V. Tešević, I. Čabarkapa, M. Todosijević, Ind. Crop. Prod. 154 (15) (2020) 112752.
- [39] D. F. Fletcher, D. D. McClure, J. M. Kavanagh, G. W. Barton, App. Math. Model. 44 (2017) 25-42.
- [40] K. Schügerl, J. Lücke, U. Oels, Adv. Biochem. Eng. 7 (1977) 1-84.
- [41] G. Keitel, Untersuchungen zum Stoffaustausch in Gas-Flüssig-Dispersionen in Rührschläufen reaktor und Blasensäule, 1978. Universität Dortmund, Dortmund, Germany (PhD Thesis).
- [42] P. S. Kojić, S. S. Popović, M. S. Tokić, I. M. Šijački, N. L. Lukić, D. Z. Jovičević, D. L. Petrović, Braz. J. Chem. Eng. 34 (2017) 493-505.
- [43] P. S. Kojić, I. M. Šijački, N. L. Lukić, D. Z. Jovičević, S. S. Popović, D. L. Petrović, Chem. Ind. Chem. Eng. Q. 22(3) (2016) 275-284.
- [44] P. S. Kojić, M. S. Tokić, I. M. Šijački, N. L. Lukić, D. L. Petrović, D. Z. Jovičević, S. S. Popović, Chemical Engineering and Technology, 38(4) (2015) 701-708.
- [45] Z. Erbay, F. Icier, J. Food Eng. 91(4) (2009) 533-541.
- [46] T. Turanyi, A.S. Tomlin, Analysis of Kinetics Reaction Mechanisms. (Springer, Berlin Heidelberg) (2014).

PREDRAG KOJIĆ <sup>1</sup>  
JOVANA KOJIĆ <sup>2</sup>  
MILADA PEZO <sup>3</sup>  
JELENA KRULJ <sup>2</sup>  
LATO PEZO <sup>4</sup>  
NIKOLA MIRKOV <sup>3</sup>

<sup>1</sup> Univerzitet u Novom Sadu,  
Tehnološki fakultet Novi Sad, Novi  
Sad, Srbija

<sup>2</sup> Univerzitet u Novom Sadu, Institut  
za prehrambenu tehnologiju, Novi  
Sad, Srbija

<sup>3</sup> Univerzitet u Beogradu, Odeljenje  
za termotehniku i energetiku, Institut  
za nuklearne nauke "Vinča" -  
Nacionalni institut Republike Srbije

<sup>4</sup> Univerzitet u Beogradu, Institut za  
opštu i fizičku hemiju, Beograd,  
Srbija

## NUMERIČKA STUDIJA HIDRODINAMIČKOG I MASENOG TRANSFERA U SPOLJNOM KRUGU AIRLIFT REAKTORA

Cilj ove studije bio je istraživanje hidrodinamičkih i maseno-prenosnih karakteristika airlift reaktora sa spoljnom recirkulacijom (ELAR). ELAR je ispitana za tri slučaja: za različite ulazne brzine gasa, za različite rastvore alkohola (voda, 0,5% metanol, 0,5% etanol, 0,5% propanol i 0,5% butanol) i za različite koncentracije metanola u rastvorima (0%, 0,5%, 1%, 2% i 5%). Proučavan je uticaj ulazne prividne brzine gasa i uticaj različitih vrsta razređenih rastvora alkohola na hidrodinamiku i koeficijent prenosa mase gas-tečnost ELAR-a. Eksperimentalne vrednosti sadržaja gasa, brzine tečnosti i koeficijenta prenosa mase u ulaznoj i silaznoj cevi su preuzete iz literaturnih izvora.

Razvijen je matematički model zasnovan na numeričkoj mehanici fluida (CFD), primenjen na dvofazno strujanje, a istraživane su različite tečnosti u pogledu površinskog napona, primenjujući metodu konačnih zapremina, Eulerov-Eulerov model i jednačine za idealan gas. Koeficijent zapreminskog prenosa mase i vrednosti za sadržaj gasa određene su CFD modelom, kao i modelom veštačke neuronske mreže. Ispitivani su uticaji parametara tečnosti i brzine gasa na karakteristike prenosa mase u sistemu gas-tečnost. Razvijeni modeli su upoređeni sa odgovarajućim eksperimentalnim rezultatima.

Ključne reči: airlift reaktor, hidrodinamika, prenos mase, Eulerov-Eulerov model, model veštačke neuronske mreže.

NAUČNI RAD